AD-A195 561 FUEL STRUCTURE AND PRESSURE EFFECTS ON THE FORMATION OF SOOT PARTICLES IN... (U) PENNSYLVANIA STATE UNIV UNIVERSITY PARK DEPT OF MECHANICAL EN... R J SANTORO

UNCLASSIFIED 15 FEB 88 AFOSR-TR-88-0664 AFOSR-87-0145 F/G 21/2 NL

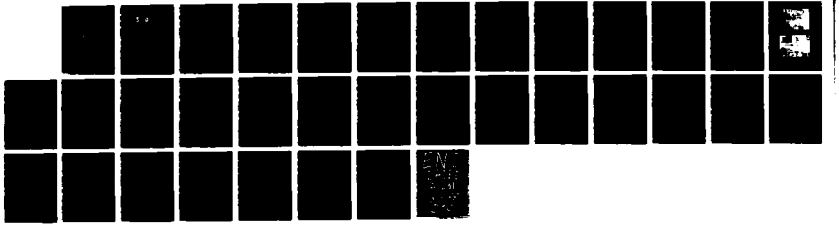

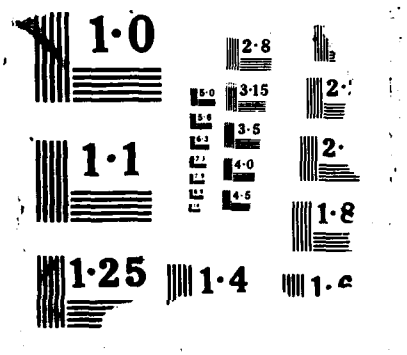
1·0
1·1
1·25
1·4
2·8
3·15
3·5
4·0
4·5
2·
1·8

(2)

AD-A195 501

DOCUMENTATION PAGE DTIC FILE COPY

Form Approved OMB No. 0704-0188

1b. RESTRICTIVE MARKINGS

2a. SECURITY CLASSIFICATION AUTHORITY

3. DISTRIBUTION/AVAILABILITY OF REPORT
Approved for public release; distribution is unlimited.

2b. DECLASSIFICATION/DOWNGRADING SCHEDULE

DTIC ELECTE JUN 30 1988 D

4. PERFORMING ORGANIZATION REPORT NUMBER(S)

5. MONITORING ORGANIZATION REPORT NUMBER(S)
AFOSR-TR- 88-0664

6a. NAME OF PERFORMING ORGANIZATION
The Pennsylvania State University

6b. OFFICE SYMBOL (If applicable)

7a. NAME OF MONITORING ORGANIZATION
AFOSR/NA

6c. ADDRESS (City, State, and ZIP Code)
University Park, PA 16802

7b. ADDRESS (City, State, and ZIP Code)
Building 410, Bolling AFB DC 20332-6448

8a. NAME OF FUNDING/SPONSORING ORGANIZATION
AFOSR/NA

8b. OFFICE SYMBOL (If applicable)
NA

9. PROCUREMENT INSTRUMENT IDENTIFICATION NUMBER
AFOSR-87-0145

8c. ADDRESS (City, State, and ZIP Code)
Building 410, Bolling AFB DC 20332-6448

10. SOURCE OF FUNDING NUMBERS

PROGRAM ELEMENT NO.	PROJECT NO.	TASK NO.	WORK UNIT ACCESSION NO.
61102F	2308	A2	

11. TITLE (Include Security Classification)
(U) "Fuel Structure and Pressure Effects on the Formation of Soot Particles in Diffusion Flames"

12. PERSONAL AUTHOR(S)
Robert J. Santoro

13a. TYPE OF REPORT	13b. TIME COVERED	14. DATE OF REPORT (Year, Month, Day)	15. PAGE COUNT
Annual	FROM 1/15/87 TO 1/15/88	1988, February, 15	29

16. SUPPLEMENTARY NOTATION

17. COSATI CODES			18. SUBJECT TERMS (Continue on reverse if necessary and identify by block number)
FIELD	GROUP	SUB-GROUP	Soot Formation, Soot Particles, Diffusion Flames

19. ABSTRACT (Continue on reverse if necessary and identify by block number)

During the first year of the present grant, efforts have concentrated on examining the effects of fuel molecular structure on soot formation in diffusion flames. Studies involving alkane, alkene, alkyne and aromatic fuel species have been studied with specific attention given to the surface growth process. Analysis of these studies has demonstrated a strong fuel structure dependence for the amount of soot formed, the conversion percentage of fuel carbon to soot, and the soot particle surface area present in these diffusion flames. However, when surface area is taken into account, similar specific surface growth rate coefficients are observed for all the fuels studied. These results point to a similar surface growth process for all the fuels. Consistent with premixed flame results, the present studies show a continual decrease in this specific surface growth rate coefficient with time. Other effects of fuel structure observed include an acceleration of the inception of soot particles to lower locations and, thus, earlier times in the flame as soot conversion percentage increases. These results also point to the importance of the initial particle inception process which appears to control subsequent soot particle evolution.

20. DISTRIBUTION/AVAILABILITY OF ABSTRACT
☒ UNCLASSIFIED/UNLIMITED ☒ SAME AS RPT ☐ OTIC USERS

21. ABSTRACT SECURITY CLASSIFICATION
Unclassified

22a. NAME OF RESPONSIBLE INDIVIDUAL
Julian M Tishkoff

22b. TELEPHONE (Include Area Code)
(202) 767-4963

22c. OFFICE SYMBOL
AFOSR/NA

DD Form 1473, JUN 86 Previous editions are obsolete. SECURITY CLASSIFICATION OF THIS PAGE

Unclassified

Annual Report

on

Fuel Structure and Pressure Effects on the Formation of Soot Particles in Diffusion Flames

(AFOSR Contract AFOSR-87-0145)

Prepared by

Robert J. Santoro
Department of Mechanical Engineering
The Pennsylvania State University
University Park, PA 16802

Submitted to:

Air Force Office of Scientific Research
Bolling Air Force Base
Washington, D.C.

February 1988

TABLE OF CONTENTS

SUMMARY

During the first year of the present grant, efforts have concentrated on examining the effects of fuel molecular structure on soot formation in diffusion flames. Studies involving alkane, alkene, alkyne and aromatic fuel species have been studied with specific attention given to the surface growth process. Analysis of these studies has demonstrated a strong fuel structure dependence for the amount of soot formed, the conversion percentage of fuel carbon to soot, and the soot particle surface area present in these diffusion flames. However, when surface area is taken into account, similar specific surface growth rate coefficients are observed for all the fuels studied. These results point to a similar surface growth process for all the fuels. Consistent with premixed flame results, the present studies show a continual decrease in this specific surface growth rate coefficient with time. Other effects of fuel structure observed include an acceleration of the inception of soot particles to lower locations and, thus, earlier times in the flame as soot conversion percentage increases. These results also point to the importance of the initial particle inception process which appears to control subsequent soot particle evolution.

In addition to these studies, significant progress has been made in the assembly and testing of the experimental facilities used in these studies. Both atmospheric and high pressure diffusion flame facilities have been assembled along with the supporting laser light scattering diagnostics. The atmospheric facility was utilized in the above experiments while the high pressure facility has recently been completed.

1. INTRODUCTION

Recent interest in the formation of soot in combustion processes has been motivated by several related developments. It is now well recognized that future combustion systems will operate with broader specification fuels under conditions of higher operating pressures and stricter emissions standards. Each of these developments requires appropriate optimization of combustion processes and system performance capabilities; increase soot formation represents a major challenge in this process. Since soot production has been shown to have strong sensitivity to fuel properties and operating conditions (temperature and pressure) [1,2], it would be desirable to have an understanding of the fundamental processes governing soot formation and subsequent oxidation. However, such understanding must also be developed under conditions which can be directly extended to processes occurring in practical combustion systems. The objective of the present effort is to investigate the effects of fuel molecular structure and operating pressure on the rates of soot formation, particle growth and burnout in a well characterized flow field. These results are expected to provide an understanding of the fundamental processes involved in soot formation under conditions which are characteristic of practical combustion systems.

2. RESEARCH OBJECTIVE

The objective of the present study is to provide an understanding of the effects of fuel molecular structure and operating pressure on the formation of soot particles in combustion systems. These studies will be carried out in a series of laminar diffusion flames and require extensive characterization of the particle, velocity and temperature fields present in these flames. Studies will be conducted at both atmospheric and elevated pressures in order to examine the effect of pressure on both the formation and oxidation of soot particles. A coannular diffusion flame apparatus is used to study the soot formation processes in these gaseous flames. The coannular burner has been selected as the experimental burner because of its demonstrated capability to produce stable flames over a wide range of operating conditions [3,4,5]. Pressure is known to exert a significant effect on soot particle formation. High pressure flame studies will be carried out in a flame facility assembled for this work which has the capability to operate at pressures as high as twenty atmospheres.

The effect of fuel structure is to be studied by the addition of aliphatic hydrocarbons (e.g., butane, butene, butadiene) and aromatics (e.g., alkylated benzenes, naphthalenes and naphthenes) in various proportions to well characterized diffusion flames. Effects of such characteristic compounds are examined using previously well characterized ethene and methane diffusion flames. These efforts can be supplemented with studies of prevaporized fuels (e.g., pentane, decane) and include blends with characteristic aromatic species. The effect that temperature has on soot formation and oxidation will also be investigated in these flames. Inert species (e.g., nitrogen and argon) can be added to either the fuel or oxidizer flow to vary the effective flame temperature. Previous studies using this approach have established the strong sensitivity of soot particle formation and destruction processes to temperature [4,6]. Using the measured particle volume fraction, size and number density, it will be possible to examine the temperature dependence of the rates of initial formation, growth and subsequent oxidation of the soot particles.

The measurement approaches stress the use of non-intrusive optical diagnostic techniques. Laser based techniques, such as laser light scattering and laser anemometry, are used to measure physical properties of the soot particles and to characterize the fluid velocity field.

At present, fine wire thermocouple measurements are used to determine the temperature field. As suitable non-intrusive techniques presently under development become available, they will be applied to the present studies.

The essential thrust of this research effort is to obtain soot particle formation, growth and burnout rates using non-intrusive techniques so as to leave unaltered the dynamic coupling of the chemical and fluid mechanical processes. The operating conditions of the flames studied and fuels investigated are intended to be characteristic of the conditions to be encountered in future gas turbine systems. The consideration of gaseous and prevaporized fuels avoids the complications that spray combustion diagnostics introduce to the study of soot formation, while preserving the consideration of realistic fuel constituents in the study. Such studies should complement work being undertaken to elucidate chemical precursor mechanisms as well as those concerned with more global measurements of soot production such as soot mass yield.

The detailed nature of the results of this study, as well as the tractable nature of the flame environment, will provide an important addition to the data base available for combustion model validation. As an approach to this aspect of the problem, a concurrent modeling effort will be undertaken to consider coupled fluid mechanic and chemical kinetic rate processes important to soot particle formation and growth.. Our approach will be to use existing models developed for conditions appropriate for laminar diffusion flames [7] and build on their capabilities to include the important particle processes [8]. Particular attention will be given to incorporating particle nucleation, surface growth, coagulation and oxidation. Efforts will also be made to collaborate with modeling approaches being attempted elsewhere [9]. Since the proposed experiments will consider a range of chemical structures under varying pressure and temperature conditions, this work will offer an opportunity for model development over a wide range of conditions.

3. ACCOMPLISHMENTS AND STATUS OF WORK

During the first year of the present grant, progress has been made in a number of areas. A brief summary of these accomplishments and current status of the present effort is given below. This summary is followed by a more detailed presentation of the progress achieved to date.

Over the past year, our research efforts have concentrated on assembly of the required apparatus as well as initiation of the soot formation studies. The following tasks have been accomplished:

(1) The atmospheric diffusion flame facility has been completed and tested.

(2) The high pressure flame facility has been designed and constructed and is presently being tested.

(3) The laser light scattering apparatus has been assembled and tested.

(4) A series of baseline studies have been completed for methane and ethene atmospheric diffusion flames. The results of the ethene flames have been compared to previous studies to assure that proper operation of the experimental facilities has been achieved. These flames have also been used as baseline comparison flames for a series of fuel addition studies.

(5) Fuel addition studies have been undertaken for methane, ethene, propene, butane, butene and butadiene fuel species. These studies have been used to examine the degree of conversion of fuel carbon to soot as a function of fuel flow rate and molecular structure. Additionally, comparisons between the methane and ethene baseline flames have provided a basis for examining potential synergism between the baseline fuel and the fuel species added to the flame.

(6) Previously completed studies of ethene, propene, butene and toluene fuel addition studies have been further analyzed. Specific attention has been given to fuel structure effects on the surface growth process. These results indicate that the specific surface growth rate coefficients are similar in magnitude for all the fuels studied, even though the available surface area varies strongly with fuel species. The magnitude of the specific surface growth rate coefficient is comparable to that observed in premixed flames.

In the sections which follow, these results will be discussed in detail. Based on this current status, implications for future work will be examined.

3.1 Atmospheric Diffusion Flame Facility

The atmospheric diffusion flame facility was completed during the first quarter of the year along with the basic laser light scattering apparatus. This facility is the major experimental apparatus used for the experiments conducted this year and a brief description of the burner facility follows.

The atmospheric diffusion flame facility consists of coannular diffusion flame burner, burner chimney, positioning system and gas metering system. The burner has a coannular configuration consisting of a 1.1 cm fuel tube surrounded by a 10 cm air annulus. The air passage is partially filled with glass beads followed by a series of fine screens to provide flow conditioning. A ceramic honeycomb 2.54 cm in thickness is used at the exit to provide a uniform flow field. The fuel tube which extends 4.8 mm above the ceramic honeycomb also is partly filled with glass beads to condition the flow. The fuel flow can consist of up to three gases, each metered with a separate rotameter. This allows for mixtures of fuels as well as nitrogen dilution of the fuel for temperature control. These rotameters have been calibrated for various gases using a soap bubble meter technique. The air flow is metered using a mass flowmeter which can monitor flows up to 5 SCFM of air. To protect the flame from room disturbances, a metal chimney has been incorporated into the burner facility. This chimney translates horizontally with the burner while sliding vertically within the chimney. Slots machined in the chimney provide for optical access.

The burner is mounted on a pair of motorized translating stages which provide for vertical and horizontal motion. A manual translation stage is also included to allow for adjustment in the second horizontal direction and is used to align the burner with the laser scattering system. The motorized stages are used to traverse the burner through the laser beam to obtain measurements over the cross section of the flame at a particular height in the flame. The motorized translation stages have a positioning resolution of 0.0127 mm which is sufficient for the present experiments. Both motorized stages are interfaced to and controlled by an IBM-XT computer using the general purpose interface bus (GPIB-IEEE 488). The software to control the translation stages is incorporated into the data acquisition program for the laser scattering measurements.

3.2 High Pressure Diffusion Flame Facility

In order to provide for studies at elevated pressure, a high pressure diffusion flame facility has been designed and constructed. This facility is composed of a coannular burner,

pressure vessel, positioning system and gas metering apparatus. The design chosen provides for a significant degree of similarity between the atmospheric and high pressure diffusion flame burners. In the present system, a burner identical to that previously described in section 3.1 has been constructed. This burner is mounted inside a high pressure vessel capable of withstanding the required operating pressures. Before describing this pressure vessel, the positioning system for the burner will be described.

Because of the mass of the pressure vessel, the approach chosen for the atmospheric system of vertically translating the entire burner and pressure vessel is not feasible. Rather the burner is mounted on a motorized translation stage located internal to the pressure vessel. Electrical connections are made through the base of the pressure vessel allowing external control of the burner's vertical position. To provide horizontal movement, the base of the pressure vessel is attached to a precision ball bearing stage which requires only a few pounds of force to move horizontally with weights as large as 1500 pounds attached. Thus, a relatively small motorized translation stage can be used to provide horizontal movement. As with the atmospheric burner, these motorized stages are capable of computer control using the laboratory IBM-XT personal computer. The only disadvantage with its approach is that sufficient space must be provided within the pressure vessel to house the vertical motion assembly and the flexible gas supply lines for the burner.

To accommodate this approach, the pressure vessel has been constructed as two separate sections. A drawing of the lower section is shown in figure 1. This section is constructed of 8 inch diameter schedule 40 carbon steel seamless pipe which is 24 inches in length. A 2 inch diameter schedule 40 carbon steel pipe is mounted and welded to this section to mount a diaphragm burst disc assembly. The burst disc is one of several safety features incorporated into the design of the burner. The vertical translating mechanism is mounted to the base of this lower section which is constructed of an 8 inch (300 lb class) blind flange. In addition to the electrical connection for the motorized translation stage, provisions for connection of fuel and air lines are also made through this flange. Internal connections to the diffusion flame burner can be made with low pressure tygon tubing since no pressure difference exists across the tubing wall inside the pressure vessel. With the upper section removed, access to the burner is easily afforded.

The upper section of the pressure vessel is shown in figure 2. This section which provides for optical access to the flame region, is 30 inches in length and is constructed from schedule XX 6 inch diameter carbon steel pipe. The wall thickness afforded by schedule XX pipe (0.864 inches) is required because of the four large diameter windows mounted into this section. These windows are two inches in diameter and 1/2 inch thick. These large diameter windows allow sufficient optical access for both the laser light scattering and the laser velocimetry measurements. In addition to the windows, access has been provided to allow igniting the flame through a 1/2 inch NPT hole in the bottom of this section. Near the top, 1/4 inch NPT holes are provided to monitor the temperature and pressure.

The operating pressure in the burner is adjusted presently using manual valves located in the exhaust line of the burner. Connection to this exhaust system is made through a second blind flange to which a 2 inch diameter exhaust line has been connected. Presently consideration is being given to replacing this manual system with a back pressure regulator which allows for better pressure control. At this time, no cooling is required for the burner or exhaust section. Temperature measurements indicate that for conditions typical for the present experiments, the burner does not heat up significantly.

Control and measurement of the fuel and air flow rates is accomplished using mass flow meters and controllers. These meters are insensitive to the operating pressure and thus can be calibrated at atmospheric pressure while providing accurate metering at elevated pressure.

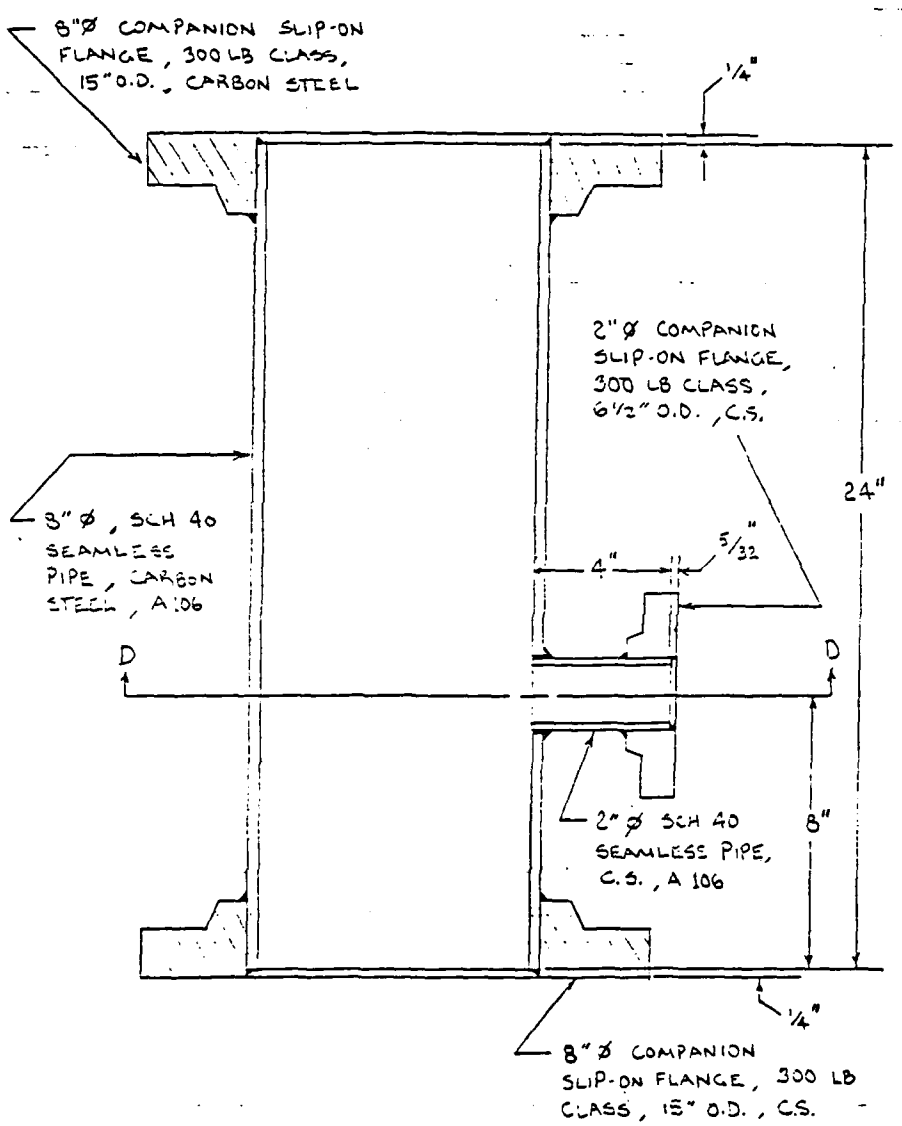

Figure 1

Drawing of the lower section of the high pressure burner.

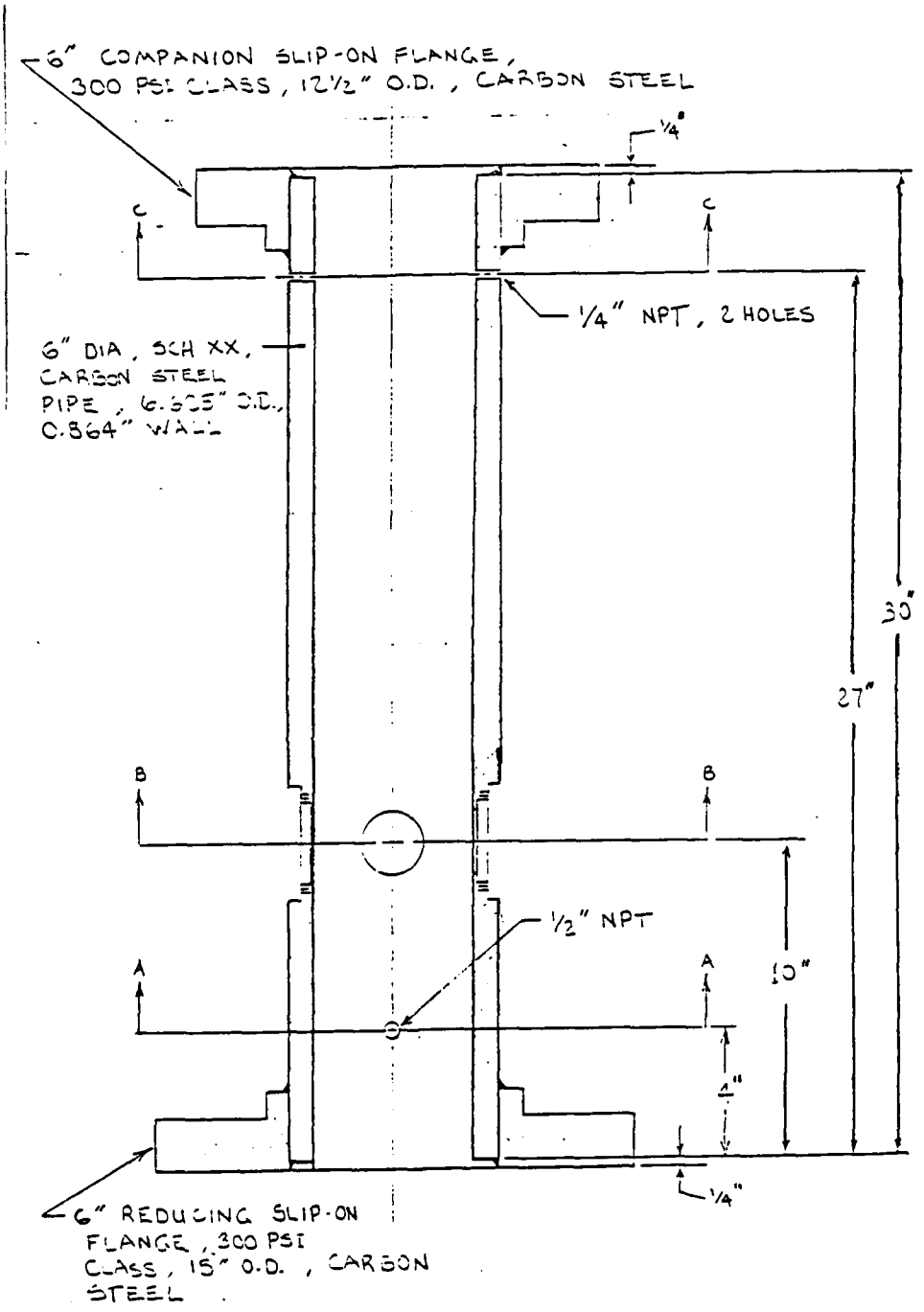

Figure 2

Drawing of the upper section of the high pressure vessel.

The fuel metering system allows up to three gases to be mixed using independent mass flow controllers. These controllers maintain a constant mass flow independent of the pressure drop across the meter. This assures a constant mass flow rate of fuel as well as a convenient start-up capability. Otherwise, the fuel flow rate would decrease as the operating pressure was increased, requiring continual readjustment. Because of the relatively large air flow rate required, a mass controller approach is not feasible for the air metering. The air flow rate is monitored by a mass flowmeter which will require adjustment as the operating pressure is varied.

The high pressure burner facility has been statically tested to 400 psig. The present laboratory air supply facilities are capable of operation to 300 psig. The burner is presently being tested under atmospheric conditions while final installation of the burner is being completed. Figures 3 and 4 show recent photographs of the high pressure diffusion flame burner. The first experiments will involve high pressure flame studies using ethene and methane as fuel. These studies will provide the baseline studies for the fuel addition studies, similar to the atmospheric studies described in sections 3.5 and 3.6.

3.3 Laser Light Scattering Apparatus

The laser light scattering apparatus, utilizing a 4W argon ion laser as the light source, provides for particle extinction and scattering measurements. Scattering measurements are presently made primarily at 90° although the system can be used to obtain measurements at 45° and 135°. The laser source is modulated using a mechanical chopper operating at 1 kHz to allow for synchronous detection of the transmitted and scattered light signals. A polarization rotator is also incorporated in the system to allow adjustment of the polarization of the incident light beam. The laser beam is focused in the burner using a 30 cm focal length lens which results in a probe beam diameter of 0.02 cm. Typically the laser is operated at the 514.5 nm laser line with an output power of about 0.5W.

The transmitted light signal is detected using a silicon photodiode. The laser light intensity is reduced by a neutral density filter (N.D. 2.0) to a level suitable for linear photodiode response. The scattered light is detected using a photomultiplier detector (PMT). The PMT has a narrowband filter center at 514.5 nm with a 1 nm bandwidth incorporated in the PMT housing to help reject light other than that generated from the particle scattering event. A pinhole with a diameter of 1 mm located in front on this filter limits the measurement volume length along the beam to 0.1 cm. The 15 cm focal length collection lens used to focus the scattered light onto the PMT, is arranged to provide unity magnification. Thus, the collection volume is a cylinder approximately 0.02 cm in diameter and .1 cm in length resulting in a volume of 3.1×10^{-3} cm^3. The collection lens is preceded by a polarization filter to allow polarization discrimination for the scattered light detected. The collection solid angle is determined by a 1.27 cm aperture which is located between the polarization filter and the collection lens. This aperture limits to the collection angle to approximately 2°.

The output from each of the detectors is input into separate two phase lock-in amplifiers which are interfaced to the IBM-XT computer over the GPIB bus. These units are capable of full computer control which allows for autoranging of the lock-in amplifiers. Computer software to control the lock-in amplifiers has been integrated with the stepper motor control programs to provide a complete data acquisition routine. These procedures provide a high degree of user independent data acquisition.

Data taken from the lock-in amplifiers is stored on the IBM-XT internal disk. The light scattering measurements require extensive data reduction to yield particle size information. Such calculations are performed more expeditiously on computers more capable than the

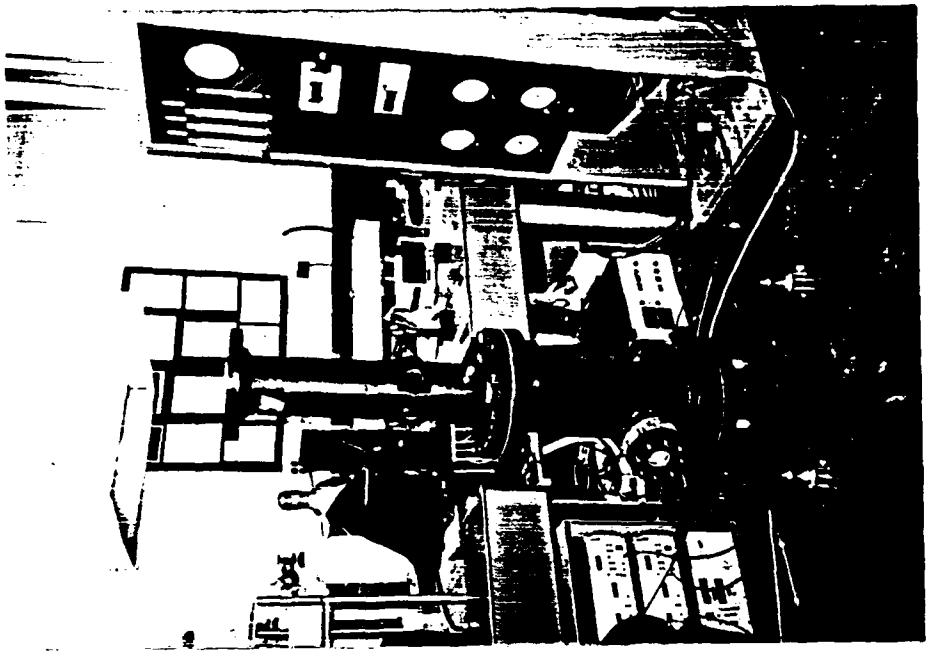

Figure 3

Photograph of high pressure diffusion flame burner.

Figure 4

Close-up view of high pressure diffusion flame burner.

laboratory computer used for the data acquisition. Thus, the IBM-XT is linked over the Mechanical Engineering Department's network to the University's VAX computer facilities. This allows for rapid data analysis and graphical output. The necessary data reduction and plotting software have been developed for this facility. In addition, the latest version of the NASA Equilibrium code has also been implemented on the VAX computer. The equilibrium program is used to calculate the adiabatic flame temperature for the diffusion flame studies.

The scattered light detection system is calibrated to account for effects of the incident laser power, sample volume, light collection efficiency, photomultiplier sensitivity and electronic gain of the system. The calibration is accomplished by passing ethene, a gas with a known Rayleigh scattering cross section, through the fuel passage of the burner and measuring the resulting scattered light. This procedure allows for an absolute determination of the differential scattering cross section per unit volume, $Q(\theta)$, which is the power scattered in the direction θ per unit incident flux. For these calibrations the incident laser beam is vertically polarized and θ is usually 90°.

The laser light scattering and extinction apparatus provides the particle measurement capability for the present studies. Analysis of the scattering measurements is based on a MIE theory approach for spherical particles. For completeness, a brief review of the theoretical basis for this analysis is presented. The present data reduction programs mentioned earlier incorporate the approach described below to obtain particle size and concentration information.

In general, the interaction of a particle and light wave is dependent on:

1. index of refraction of the particle, m
2. particle size, D
3. particle number density, N
4. particle size distribution, P(D)
5. particle shape
6. wavelength of the scattered light
7. scattering geometry

Obviously, measurement of any one of the above requires knowledge of all of the other variables. In a typical combustion measurement of soot particles, only the scattering geometry and the wavelength of the light can be specified beforehand. The remaining unknowns are determined by an appropriate combination of measurements to reduce the number of free parameters along with some reasonable assumptions. It is these assumptions which can result in inaccuracies and therefore must be considered carefully.

Combinations of scattering measurements utilizing the angular and polarization dependencies of the scattering process, or scattering and absorption measurements, have been used to determine particle number density and size [3-5]. In such an approach, the index of refraction is taken to be known, the particles are assumed to be spherical and a size distribution is assumed (e.g., log-normal).

The determination of particle size and number concentration from light scattering data depends primarily on our capability to relate the measurement of scattered and absorbed light intensity to the particle properties. Appropriate theories have been developed for spherical

particles and have been widely applied for aerosol measurements. The particle properties of interest are the differential scattering cross section, $C_{ij}(\theta)$, for production of scattered light at a specified direction and total cross section for a specified particle size, C_{ext}. The subscripts i and j for the scattering cross section assume letters v or h according to whether the state of polarization of the scattered (i) and incident (j) radiation is perpendicular or parallel, respectively, to the plane of observation. For spherical particles of isotropic material, only the case of i = j is of interest because cross polarization effects are absent.

The relationship between these cross sections and the experimentally measured quantities are expressed as

$$I_s = I_0 N C_{ii} \left(\theta, \frac{\pi D}{\lambda}, m\right) G \tag{1}$$

and

$$\frac{I}{I_0} = \exp - \int_0^L N C_{ext} \left(\frac{\pi D}{\lambda}, m\right) ds \tag{2}$$

where I_s, I and I_0 are the scattered, transmitted and incident intensities respectively, N is number concentration of particles, D is diameter, m is the refractive index, and G is a constant which involves factors related to the sample volume and detection instrumentation. It should be noted that the scattering cross section measurements given by equation (1) are point measurements, while the extinction cross section is an integrated quantity over the path length L. Thus, to obtain local particle extinction values, a data inversion technique must be utilized [10].

In an experiment, the quantities which are determined, once appropriate calibration factors have been introduced, are

$$Q_{ii} = N C_{ii} \tag{3}$$

and

$$K_{ext} = N C_{ext} \tag{4}$$

where Q_{ii} is the volumetric scattering cross section and K_{ext} is the extinction coefficient.

Several approaches can be taken to determine the particle size from the above defined cross sections. Three are of interest with respect to the instrumental set up discussed previously. These are the ratio of scattering to extinction, $Q_{vv}(90°)/K_{ext}$, the ratios of the scattering signal at two angles (dissymmetry ratio) $Q_{vv}(45°)/Q_{vv}(90°)$ and $Q_{vv}(45°)/Q_{vv}(135°)$, and the polarization ratio $Q_{hh}(90°)/Q_{vv}(90°)$; the scattering measurement angle is specified for each quantity. Each of these ratios have a strong dependence on particle size and represent a redundant set of data in terms of the particle properties for particles in the Mie size region ($D > \lambda$). For particles in the Rayleigh size region ($D << \lambda$), scattering is isotropic so the dissymmetry ratio has a value of unity and the defined polarization ratio approaches zero.

Thus, in this small particle limit, only the scattering/extinction ratio yields size information. However, for soot formation processes, the rapid coagulation and surface growth processes lead quickly to particles in the Mie region. Nonetheless, the scattering measurement capabilities described above, provide for the measurement of the particle size throughout the Rayleigh and Mie regimes. Thus, processes from nucleation through particle growth and eventual particle oxidation are measurable.

With the particle size established, any one of the scattering cross sections can be used to find N or f_v, the soot volume fraction. The soot volume fraction, particle size and number density are related by

$$f_v = \frac{N\pi D^3}{6} \tag{5}$$

For a system in which simultaneous nucleation, particle growth and coagulation are present, a particle size distribution can be assumed to exist. In this case, the previously defined particle scattering cross sections must be averaged over the size distribution function, P(D), to yield mean values,

$$C_{ii}(\theta) = \int_0^\infty C_{ii}\left(\theta, \frac{\Pi D}{\lambda}, m\right) P(D)\, dD \tag{6}$$

$$C_{ext}(\theta) = \int_0^\infty C_{ext}\left(\theta, \frac{\Pi D}{\lambda}, m\right) P(D)\, dD \tag{7}$$

A widely used expression for P(D) is the logarithmic normal distribution that is given by

$$P(D) = \frac{\exp\left[-(\ln D/D_g)^2/2\,\sigma_g^2\right]}{\sqrt{2\Pi}\,\sigma_g D} \tag{8}$$

where D_g and σ_g are the geometric mean diameter and geometric mean standard deviation, respectively. As is discussed in Ref. 12, the introduction of particle size distribution affords an opportunity to derive additional information by utilizing the previously redundant measurements of the scattering cross sections. These now afford the possibility of learning more about the nature of the size distribution function and agglomerate particle properties.

With the burner facilities and particle diagnostics completed, a series of soot formation studies have been undertaken. The accomplishments and status of those experiments are discussed in the next three sections.

3.4 Atmospheric Ethene and Methane Flame Studies

A series of ethene and methane flames have been studied to characterize their soot particle fields. These experiments had two major objectives. The first was to allow a comparison between the present measurements and previous results for ethene/air diffusion flames [3]. Such a comparison would assure that the atmospheric flame facility and laser light scattering system were operating properly. The second objective was to provide a baseline data set for these fuels to be used in the fuel addition studies.

To validate the operation of the atmospheric burner facility and laser light scattering system, a well characterized ethene/air diffusion flame was chosen for study. The flame conditions correspond to an ethene fuel flow rate of 3.85 cm^3/s and an air flow rate of 1.51 SCFM (716 cm^3/s). Radial profiles of the light extinction and scattering by soot particles in the flame were obtained at several axial locations. This data allow for the determination of the volume fraction, f_v, the particle diameter, D_{63}, and the particle number concentration, N. Comparisons between this data and previously published results showed good agreement. Figure 5 shows a plot of the maximum value of f_v as a function of the axial location in the flame compared to the results reported in Ref. 3. Some differences between the two experiments are observed in the region near the maximum f_v in the flame (z = 40 mm) which continue into the particle oxidation region. However, these differences are not considered critical at this time. Similar agreement has been observed for D_{63} and N.

The study of the effects of fuel molecular structure on the formation of soot is one of the major elements of the present work. However, a difficulty in studying fuel structure effects has been the wide differences in the flame size and shape which results when various fuels are burned at, for example, a characteristic condition such as the soot point. These differences result in important variations in the temperature and velocity fields which make quantitative comparisons impossible between the flames.

In the present studies, this difficulty is addressed by adopting a fuel addition approach involving well characterized baseline flames in which the soot particle field is characterized in detail. The fuel molecular structure effects are then investigated by adding an additional fuel component to the baseline flame. However, the total carbon flow rate is kept constant. This means that an appropriate fraction of the baseline fuel is replaced with the additive fuel. With the soot contribution from the baseline fuel known, the effect of the additive fuel on the formation of soot particles can be determined. Under these conditions, the flame size and shape remains similar for all flames.

Two fuels, methane and ethene, have been selected to serve as the baseline flames. The methane flames have relatively low soot particle formation and thus provide greater sensitivity for measuring changes introduced by varying the fuel molecular structure. The ethene flames represent the best studied set of diffusion flames presently available and provide a significant comparative data base. Comparisons between the two baseline systems will also provide a basis for examining potential synergistic effects between the fuel addition species and the baseline fuel. Four flames have been studied for the two fuels. The flow conditions for the flames are shown in Table 1. In order to illustrate the differences between the two baseline flames, a plot of the integrated soot volume fraction, F_v, is shown in figure 6 for three of the baseline flames. The value of F_v, which is a measure of the total amount of soot formed in the flame, is given by

$$F_v = 2\pi \int_0^R f_v \, r \, dr \tag{9}$$

where R is the radius of soot particle field. In figure 6, F_v is plotted versus a non-dimensional height, η, which is related to axial location z by

$$\eta = \frac{zD}{\dot{V}} \tag{10}$$

where D is the diffusion coefficient of the fuel and $\dot{V}$ is the volumetric flow rate of the fuel.

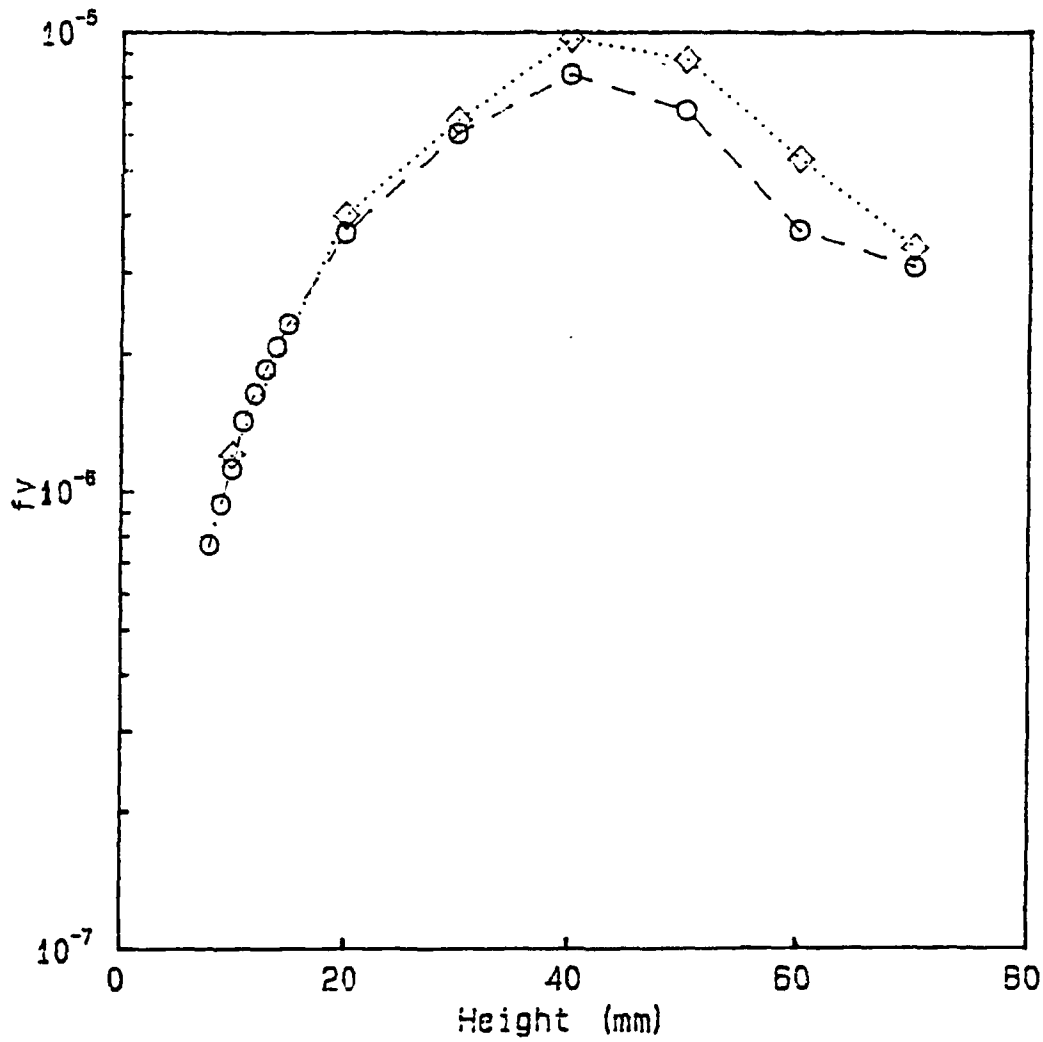

Figure 5

Comparison between the present study and the results reported in reference 3 of the maximum values of the soot volume fraction, f_V, as a function of the axial location in an ethene/air diffusion flame. Diamonds - Ref. 3, circles - present studies.

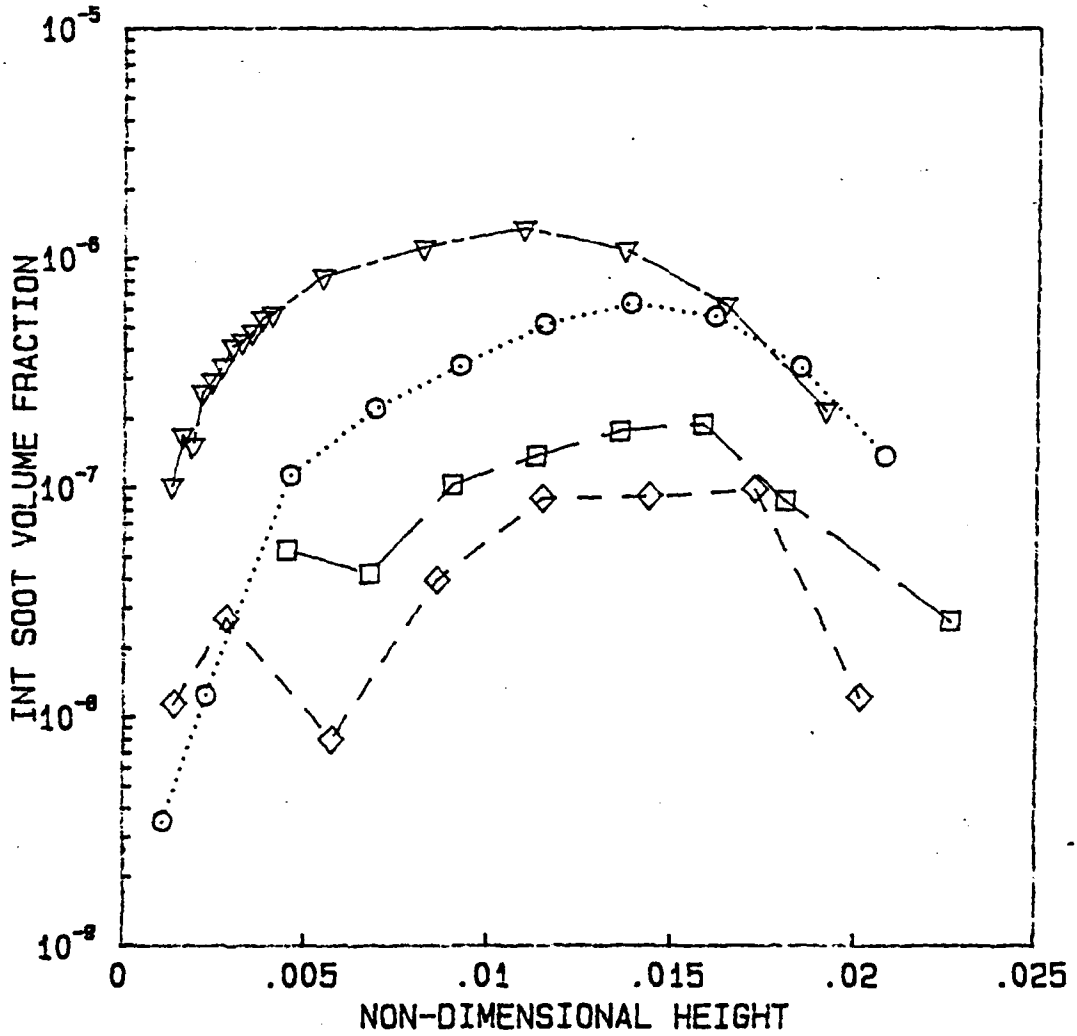

Figure 6

Comparisons of the integrated soot volume fraction, F_v, as a function of the non-dimensional height. Triangles - C_2H_4 = 3.85 cm^3/s; circles - CH_4 = 7.70 cm^3/s + C_2H_4 = 1.05 cm^3/s; squares - CH_4 = 9.8 cm^3/s; diamonds - CH_4 = 7.70 cm^3/s.

Table 1

Flow conditions for the baseline flame studies

Fuel	Fuel Flow Rate (cm^3/s)	Air Flow Rate (SCFM)
C_2H_4	3.85	1.5
C_2H_4	4.90	2.75
CH_4	7.7	2.75
CH_4	9.8	2.75

The significantly lower soot formation character of the methane flames as compared to the ethene flame is clear. To illustrate the sensitivity of the methane baseline flame to the addition of a different fuel species, the results of a flame burning a mixture of methane and ethene is also shown in figure 6. The soot particle field measurements made for these baseline flames will be utilized in the fuel addition studies. The present status of those studies is discussed in the next section.

3.5 Fuel Addition Studies

With the baseline flame studies completed, the effects of fuel molecular structure on the soot formation process has been initiated. Experiments have emphasized the methane baseline flames to date. Table 2 summarizes the flame conditions which have been studied. Previously, results have been reported for various fuels added to an ethene diffusion [13] which serve as additional data for the present studies. The experiments involving the fuel addition to methane and ethene flames have been selected to examine three effects. Specifically, the experiments are intended:

(1) To systematically examine the conversion of fuel carbon to soot as function of fuel flow rate. The experiments in which ethene or butene are added to the methane flame address this point.

(2) To investigate the relative effects of changing the fuel structure in a series of fuels which involve an alkane, alkene, and alkyne species. The experiments in which butane, butene and butadiene are added to the flame address this point.

(3) To compare the effects of the baseline fuel on the conversion of fuel carbon to soot for the fuel addition approach. Experiments in which ethene and butene have been added to both baseline flames have been utilized for this comparison.

Table 2

Flow conditions for the fuel addition studies

Baseline Fuel	Flow Rate (cm^3/s)	Fuel Added	Flow Rate (cm^3/s)	Air Flow Rate SCFM
CH_4	8.75	C_2H_4	0.525	2.75
CH_4	7.7	C_2H_4	1.05	2.75
CH_4	5.6	C_2H_4	2.10	2.75
CH_4	5.6	C_4H_8	1.05	2.75
CH_4	5.6	C_4H_8	0.872	2.75
CH_4	7.7	C_4H_8	0.525	2.75
CH_4	5.6	C_4H_{10}	1.05	2.75
CH_4	5.6	C_4H_6	1.05	2.75

The analysis which is presented below represents an initial approach to these studies. It focuses on the carbon conversion percentage for each of the flames based on the amount of fuel added to the baseline flame. The contribution of the baseline flame is subtracted from the soot present in the flame based on the studies of the atmospheric ethene and methane flames described in section 3.4. The carbon conversion percentage is calculated for the axial location displaying the maximum value of F_v, the integrated soot volume fraction. The carbon conversion percentage can be expressed as

$$\% \text{ conversion} = \frac{\dot{m}_s - \dot{m}_B}{\dot{m}_c - \dot{m}_B} \times 100 = \frac{\dot{m}_s - \dot{m}_B}{\dot{m}_{add}} \times 100 \qquad (11)$$

where $\dot{m}_s$ is the soot mass flow rate at the location of maximum F_v for the flame containing the fuel addition, $\dot{m}_c$ is the mass flow rate of carbon entering the burner, $\dot{m}_B$ is the mass flow rate of carbon contained as baseline fuel and $\dot{m}_{add}$ is the mass flow rate of carbon corresponding to the fuel species added to the flame. The determination of the soot mass flow rate at a particular height in the flame can be calculated from:

$$\dot{m}_s(z_m) = 2\pi\rho \int_0^R v(r, z_m)\, f_v(r, z_m)\, r\, dr \qquad (12)$$

where z_m is the axial location where F_v is a maximum, ρ is the density of soot and v is the velocity. Thus, the velocity profile must be known to precisely calculate the value of $\dot{m}_s$. For the present analysis, the velocity has been assumed to be independent of r with a value for axial location z_m taken from Ref. 14. This is a reasonable assumption for the locations for which F_v is observed to be a maximum [14]. With this assumption $\dot{m}_s$ can be expressed as

$$\dot{m}_s (z_m) = \rho \, v(z_m) \, F_v(z_m) \qquad (13)$$

where ρ is taken to be 1.8 gm/cm^3. Tables 3-5 tabulate the results of this analysis for several of the flames studied. Included along with the percent conversion result is the calculated adiabatic flame temperature for each flame. Each of the tables addresses one of the effects described at the beginning of this section.

Table 3

Flow conditions for the studies of the fuel flow rate effects

Baseline Fuel	Flow Rate (cm^3/s)	Fuel Added	Flow Rate (cm^3/s)	% Conversion*	T_{ad} (K)
CH_4	8.75	C_2H_4	0.525	21.5	2239
CH_4	7.70	C_2H_4	1.05	19.0	2252
CH_4	5.60	C_2H_4	2.10	16.2	2280
CH_4	7.70	C_4H_8	0.525	36.6	2242
CH_4	5.60	C_2H_8	0.872	33.3	----
CH_4	5.60	C_4H_6	1.05	35.1	2260

* ρ = 1.8 gm/cm^3

In the fuel addition approach, a fraction of the baseline is replaced with the fuel species of interest subject to the constraint that the total flow rate of carbon into the flame is maintained constant. It is of interest to ascertain if the percentage of fuel carbon converted to soot is dependent on the amount of the baseline fuel replaced. The results tabulated in Table 3 for a methane baseline flame in which ethene or butene were introduced provide information on this point. For the ethene fuel addition case, the ethene flow rate was varied by a factor 4, whereas for the butene case the flow rate was changed by a factor of 2. In the case of the butene studies, the percent conversion remained relatively constant. For the ethene case, a small systematic decrease in the conversion percentage of fuel carbon to soot is observed with increasing ethene flow rate. Consideration of the variation in the calculated adiabatic flame temperature (T_{ad}) does not explain the observed results since a decrease in the conversion percentage is opposite to the current view of the effect of temperature on soot production. It is conceivable that the observed variation in the conversion percentage is within the experimental error. A careful consideration of potential sources of error will be carried out to better resolve this question. At present, the data supports the conclusion that the conversion percentage is only weakly dependent on the fuel addition flow rate. The differences observed between species with different fuel molecular structure is significantly greater than the observed variations with

Table 4
Flow conditions for the butane, butene, and butadiene addition studies

Baseline Fuel	Flow Rate (cm^3/s)	Fuel Added	Flow Rate (cm^3/s)	% Conversion*	T_{ad} (K)
CH_4	5.6	C_4H_{10}	1.05	12.2	2243
CH_4	5.6	C_4H_8	1.05	35.1	2259
CH_4	5.6	C_4H_6	1.05	44.4	2285

* ρ = 1.8 gm/cm^3

respect to flow rate. This provides an experimental justification to extend the results of these studies to more general fuel mixture conditions.

To specifically examine the effect of fuel molecular structure on the soot formation process, a series of flames are being examined involving C_4 species. The flames studied involved additions of butane, 1-butene and 1,3-butadiene to a methane baseline flame. In this series the fuel structure is varied in terms of the arrangement of carbon bonds (single bonds and double bonds) resulting, of course, in a variation of the carbon to hydrogen ratio. Table 4 tabulates the results of these experiments in terms of conversion percentage of fuel carbon to soot. Figure 7 shows the integrated soot volume fraction, F_v, as a function of the axial coordinate, z. These results represent the most recent work undertaken and, thus, the present analysis is preliminary in nature.

Clearly, the results in Table 4 and figure 7 indicate a strong fuel structure effect with the conversion percentage more than tripling. In addition, there is a systematic decrease in the axial position where soot is first observed as the more sooty fuels are considered. This indicates that the reactions leading to the first soot particles occur more rapidly in these flames. More detailed comparisons utilizing the velocity and temperature fields should offer the potential for comparing the overall chemical kinetic rate information for the governing pyrolysis or oxidative pyrolysis mechanisms which have been established for these fuels. These velocity and temperature measurements are planned during the next phase of the project. Comparisons are also possible between the methane and ethene baseline flames to investigate the importance of the C/H ratio which will vary strongly between the two flame systems. To date, the experiments undertaken have not attempted to control temperature which has been shown to be an important parameter in the soot formation process [6]. An advantage of the fuel addition approach lies in the fact that changes in the flame temperatures between different flames are often small. However, there are cases where the temperature variation is significant enough to be important. As stated above, these studies have not yet been fully analyzed and some addition measurements are required before detailed mechanistic information will be forthcoming. However, the present results do demonstrate the fuel addition approach does allow investigation of fuel molecular effects under comparable flame conditions. This data provides unique information on the fundamental mechanisms which control the formation of soot particles in flames.

The discussion above has focused on the effects of fuel molecular structure and flow rate. An additional important consideration is the importance of the baseline fuel which is used. To examine this point, two fuel addition studies involving ethene and butene were compared in

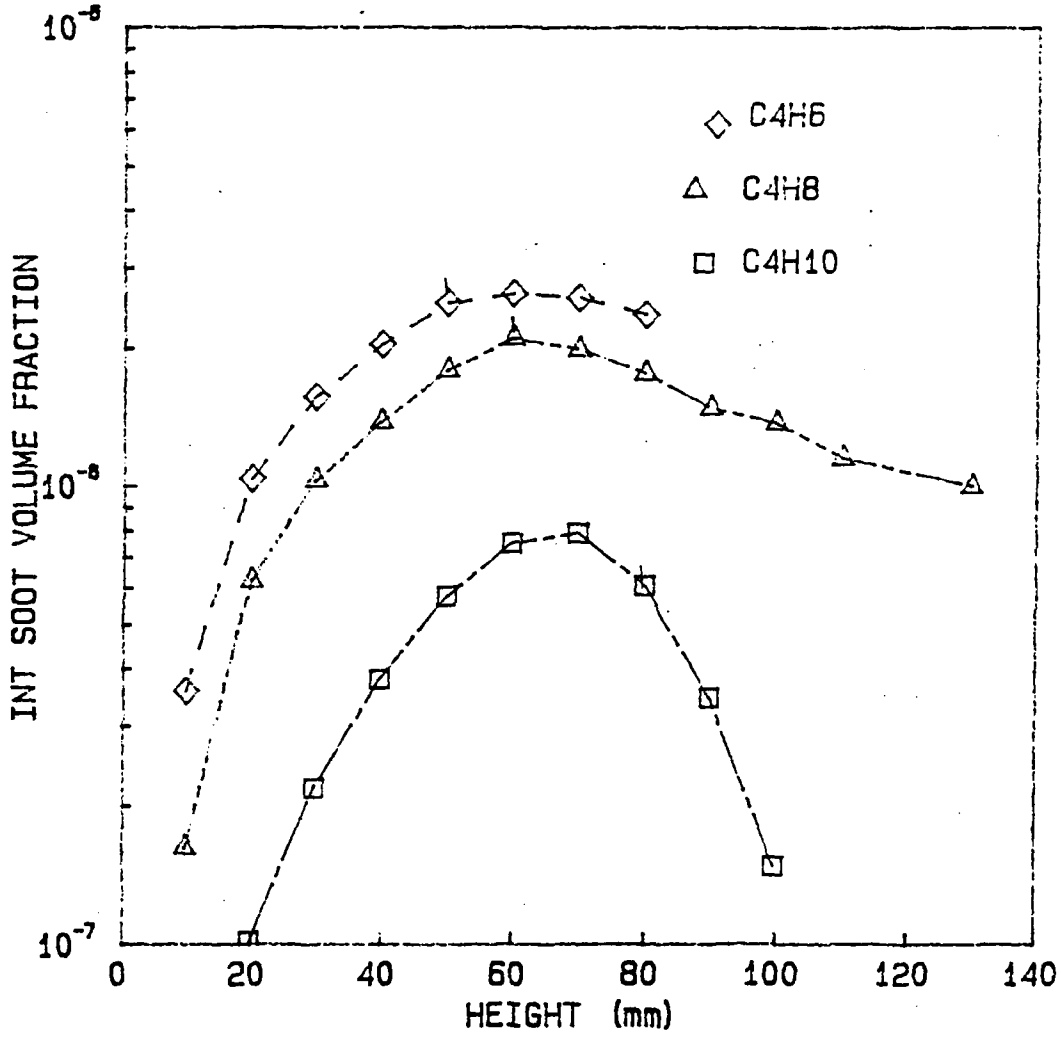

Figure 7

Comparison of the integrated soot volume fraction, F_V, for the butane, 1-butene and 1,3-butadiene fuel addition studies. The baseline flame had a methane flow rate of 5.6 cm^3/s and a fuel addition flow rate of 1.05 cm^3/s.

which the baseline fuels were varied using methane and ethene. The results of these studies in terms of conversion percentage are tabulated in Table 5.

Table 5
Flow conditions for flame studies of baseline fuel synergism

Baseline Fuel	Flow Rate (cm^3/s)	Fuel Added	Flow Rate (cm^3/s)	% Conversion*	T_{ad} (K)
CH_4	7.7	C_2H_4	1.05	19.0	2252
CH_4	7.7	C_4H_8	0.525	36.6	2242
C_2H_4	3.85	C_2H_4	1.05	16.2	2369
C_2H_4	3.85	C_4H_8	0.525	46.8	2359

*ρ = 1.8 gm/cm^3

These results, as with the flow rate results previously discussed (see Table 3), do show some sensitivity to a variation in the flame conditions. However, again, the differences are significantly smaller than the variation resulting from the fuel structure variation. For the experiments shown in Table 5, the soot conversion percentage approximately doubles for the change in fuel species. However, differences in the results for the various baseline flames for a particular fuel (ethene or butene) is typically 20-25%. It is also worth mentioning that the calculated flame temperatures vary by about 100K for the fuels studied. Thus, some of the variation may be a result of the temperature difference. The comparison between the ethene and butene results may indicate different temperature sensitivities since the observed effects of the baseline flame are reversed. This again points out the strength of the present approach to help isolate particular effects.

The above discussion has emphasized the conversion percentage of fuel carbon to soot particles. This quantity is very useful in illustrating the impact of the effect of fuel molecular structure on soot formation. However, it represents a global measurement of the soot formation process. More fundamentally significant results are realized when the detailed temperature time history characterizing these chemically reacting systems are analyzed. This more fundamental analysis of the previously describe results is one of the objectives for the current year of the program. In the next section more detailed results are presented for the surface growth process. These results more fully represent the fundamental insights and quantitative information which is possible from studies of this nature.

3.6 Fuel Molecular Structure Effects on Soot Surface Growth Processes

The formation of soot particles is now viewed to undergo a common sequence of events which govern the amount of soot formed and emitted from combustion systems. These include: (1) a chemical kinetically controlled reaction sequence which results in the formation of precursor species needed to form the first particles, (2) a particle inception stage which results in the formation of large numbers of small primary particles, (3) a particle growth period in which surface growth and particle coagulation processes contribute to the increase in particle size and (4) a stage in which material is no longer added to the soot particles and size is controlled by agglomeration or may even be reduced by oxidative attack. Recent work

in premixed flames has concentrated on more firmly establishing quantitative measurements of these processes. Significant progress has been made in understanding the surface growth and coagulation processes which occur in premixed flames [15,16]. Results of these and other studies have emphasized the importance of acetylene (C_2H_2) and the available surface area in the particle surface growth process. However, to date, little information is available on similar processes in diffusion flames.

To help resolve this situation, the surface growth process for a number of fuel species has been studied using the fuel addition approach described above. These studies were conducted using a well characterized ethene/air diffusion flame as the baseline flame. Different fuel species were added to the baseline fuel (ethene), such that the additional carbon flow rate is held constant. In addition, the flame size and shape remains similar for all the flames studied, thus minimizing changes in burner heat loss or particle transport in the flame. An ethene fuel flow rate of 3.85 cc/s (a carbon flow rate of 3.78×10^{-3} g/s) was selected for the baseline flame since this diffusion flame has been extensively studied [4,14]. A second fuel was added to the ethene flow to produce a total carbon flow rate of 4.81×10^{-3} g/s, an increase of 1.03×10^{-3} g/s from the baseline case. Results obtained for ethene, propene, butene, and toluene will be discussed. In the case of toluene, the fuel was vaporized using a technique similar to that described by Gomez, et al. [17]. The flow rate conditions, soot conversion percentages and calculated adiabatic temperatures are shown in Table 6.

Using the previously obtained detailed information on the particle paths for the ethene flame, comparisons between the different fuel mixtures can be made. For this comparison the region of the flame containing the maximum soot volume fraction will be examined. Figure 8 shows the time evolution of the soot volume fraction, f_v, along the particle path which traverses the annular region of the flame where the maximum f_v is observed. The fuel mixtures shown include three alkenes (ethene, propene and butene) and an aromatic (toluene) fuel. The calculated adiabatic flame temperatures for these fuel mixtures vary by less than 10K. Thus, the temperature fields characterizing these flames should be similar allowing a direct comparison between the flames.

The soot volume fraction is observed to reach a maximum at a similar time (60 ms) for each fuel mixture. For the alkene fuels, the observed residence time at which soot particles are first observed and the value of f_v at this time are very similar. However, the different alkene fuels are observed to have measurably different rates of growth in terms of the change in f_v with time. For the toluene mixture, although soot particles are first observed at a similar residence time (≈21 ms), the initial concentration is much higher. This implies that soot particle inception occurred at an earlier time or that the inception process is much more vigorous. The particle size and number density measurements from nearby particle paths favor an interpretation indicating an earlier inception time. Thus, these results indicate that the specific nature of the fuel species is observed to affect the initial particle formation process as well as the subsequent growth rates.

In order to examine the surface growth process in more detail, figure 9 shows the particle surface area calculated from the particle diameter and number density measurements for the region along the same particle path. For each of the fuel mixtures studied the surface area is observed to increase with time and fuel mixtures which exhibit larger soot

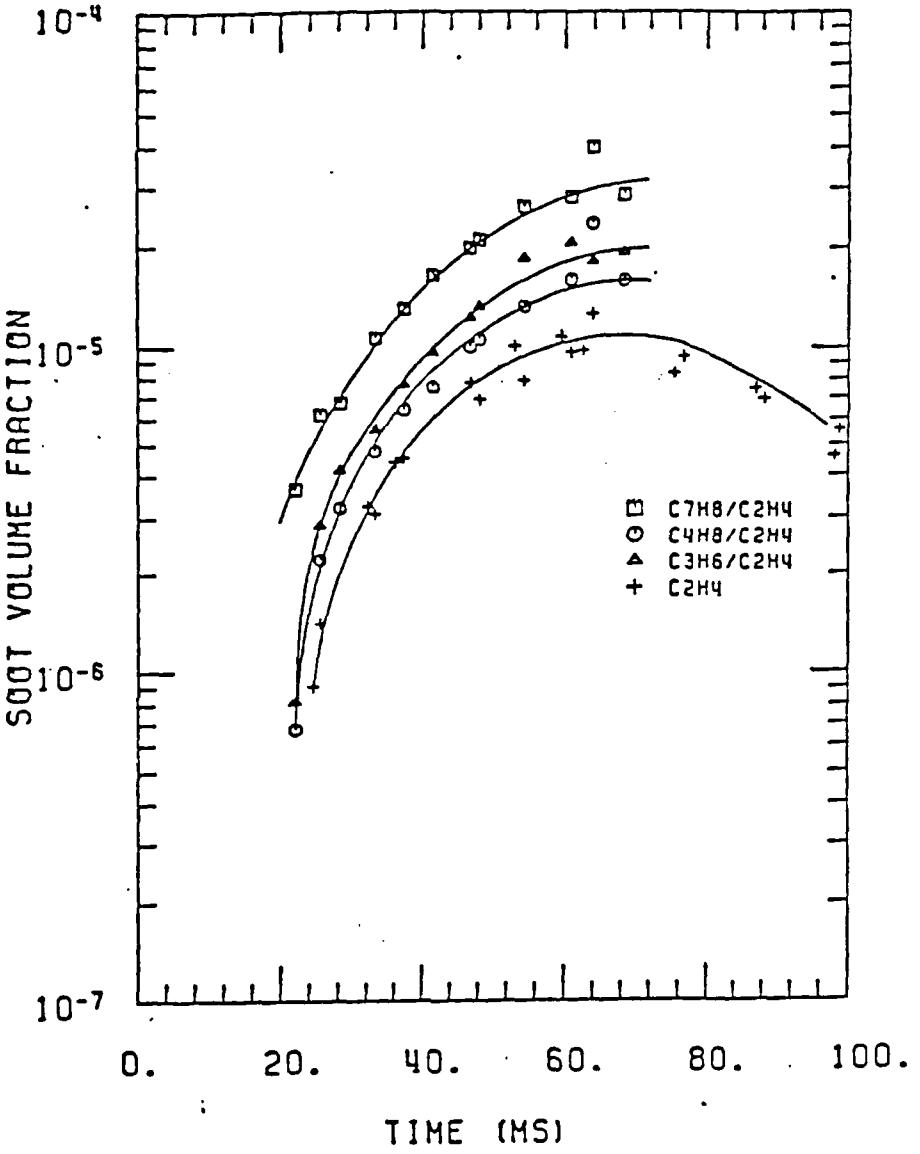

Figure 8

Comparison of the soot volume fraction along the particle path exhibiting the maximum soot volume fraction for fuel mixtures containing ethene, propene, butene, or toluene.

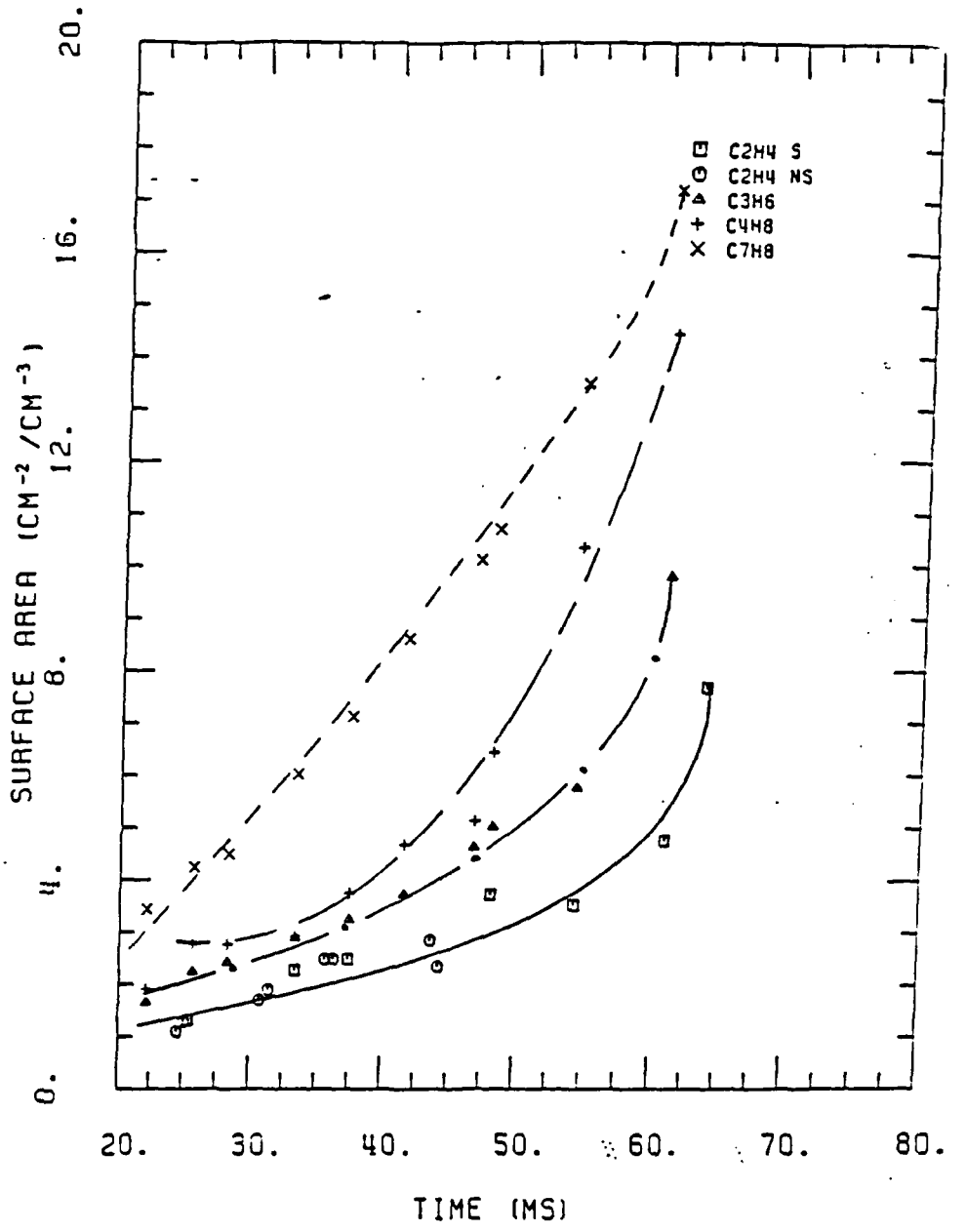

Figure 9

Soot particle surface area along the particle path exhibiting the maximum soot volume fraction for fuel mixtures containing ethene (S - 4.9 cm^3/s and NS - 3.85 cm^3/s fuel flowrate), propene, butene, and toluene.

Table 6

Baseline Fuel	Flow Rate	Fuel Added	Flow Rate	% Conversion*	T_{ad}
Flow conditions for fuel addition studies in ethene/air diffusion flames					
C_2H_4	3.85	C_2H_4	1.05	16.2	2369
C_2H_4	3.85	C_3H_6	0.70	32.4	2368
C_2H_4	3.85	C_4H_8	0.525	46.8	2359
C_2H_4	3.85	C_7H_8	0.30	88.2	2361

*ρ = 1.8 gm/cm^3

volume fractions also display greater surface area available for growth. Harris and co-workers in their studies of premixed ethene flames [15,16] have described the surface growth by

$$\frac{dM}{dt} = k\, S\, [C_2H_2] \qquad (14)$$

where M is the mass of soot in g/cm^3, k is a growth rate constant (g/cm^2 s atm), S is the surface area (cm^2) and the last term is the concentration of acetylene [atm]. In the present experiments, measurements of the acetylene concentration are not available. However a comparison of the specific surface growth rate (1/S dM/dt) can be obtained and is shown in figure 10. For these calculations, the density of soot was chosen to be 1.8 g/cm^3. Shown also on this figure are the data for an ethene premixed flame studied by Harris, et al. with a C/O ratio of 0.94. The data of Harris et al. have been offset 15 ms to allow presentation in a proper time frame for these diffusion flame studies. The resulting specific surface growth rates calculated in this manner are very similar for each of the fuel mixtures studied as shown in figure 10. Furthermore, the comparison between the diffusion flame and premixed flame studies is quite reasonable. Considering the differences in the flame environments, this agreement is very encouraging and indicates the surface growth processes in both flame systems are quite similar. It is also of interest that for the propene, butene and toluene mixtures that slightly larger rate constants are observed at the earliest times. These results emphasize the need for further study of the particle inception process which may well be controlling the evolution of the soot particle field.

3.7 Conclusions and Future Work

The results which have been presented above demonstrate the usefulness of the fuel addition studies of molecular structure effects. These experiments have provided quantitative information on the conversion of fuel to soot particles for a variety of molecular structures. The conversion percentage has been shown to be only weakly dependent on the fuel flow rate or the baseline fuel to which the additions are made. Detailed studies of the surface growth process for soot particles in diffusion flames have revealed strong similarities for the fuels studied. This suggests a common mechanism for the surface growth process which provides a significant reduction in the complexity in modeling soot formation. The present work represents the first detailed measurements providing quantitative information on these processes as a function of fuel structure.

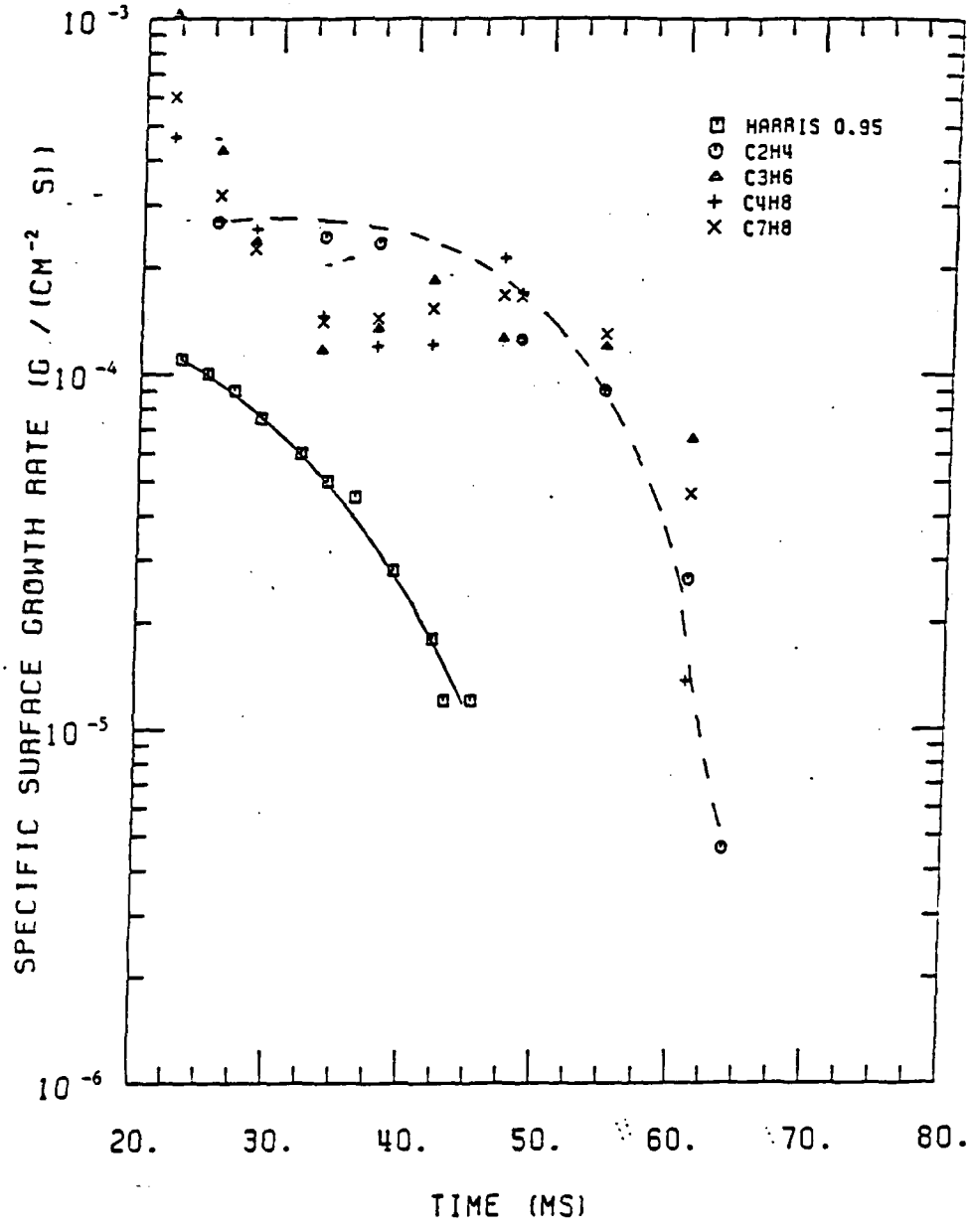

Figure 10

Specific surface growth rate along the particle path exhibiting the maximum soot volume fraction. The dashed line (---) is a best faired curve through the ethene flame results.

Based on these results, future studies will concentrate on examining in a more detailed manner the evolution of the soot particle field in diffusion flames. These studies will focus on the relationship between the known kinetic mechanisms for pyrolysis of these fuels and the sensitivity of the soot formation process to variations in the fuel molecular structure. This comparison will require velocity and temperature measurements to complement the soot particle measurements. These measurements are among the objectives for the present year. As the surface growth results indicate, the early particle formation region is critical to the evolution of the soot particle field. Additional studies will emphasize measurements in this region as a function of fuel molecular structure.

In addition to an interest in the atmospheric studies, the high pressure studies also point to several interesting features. Since the observed conversion percentages of fuel carbon to soot have shown strong fuel molecular structure sensitivity, one may similarly expect variations in the pressure sensitivity as well. Since very little research has been directed towards this topic, the present studies are an important step in providing a basis for understanding the effects of operating pressure on soot formation.

4. REFERENCES

1. Jackson, T. A., J. Energy, 6, p. 376 (1982).

2. Blazowski, W. S., Sarofim, A. F. and Keck, J. C., J. of Eng. Power, 103, p. 42 (1981).

3. Santoro, R. J., Semerjian, H. G. and Dobbins, R. A., Combustion and Flame, 51, p. 208 (1983).

4. Santoro, R. J., Semerjian, H. G., Twentieth Symposium (International) on Combustion, The Combustion Institute, Pittsburgh, PA, pp. 997-1006 (1984).

5. Santoro, R. J., Yeh, T. T. and Semerjian, H. G., in Heat Transfer in Fire and Combustion Systems, edited by C. K. Law, Y. Jaluria, W. W. Yuen, K. Miyasaka, pp. 57-69, The American Society of Mechanical Engineers, New York (1985).

6. Glassman, I and Yaccarino, P., Eighteenth Symposium (International) on Combustion, The Combustion Institute, Pittsburgh, p. 1175 (1981).

7. Mitchell, R. E., Sarofim, A. F. and Clomburg, L. A., Combustion and Flame, 37, p. 227 (1980).

8. Dobbins, R. A. and Mulholland, G. W., Combust. Sci. and Tech., 40, p. 175 (1984).

9. Davis, R. and Baum, H., Center for Chemical Engineering, National Bureau of Standards (private communication).

10. Santoro, R. J., Semerjian, H. G., Emmerman, P. J., Goulard, R., Int. J. Heat Mass Transfer, 24, pp. 1139 (1981).

11. D'Alessio, A., DiLorenzo, A., Sarofim, A. F., Beretta, A., Masi, S., And Venitozzi, C., Fifteenth Symposium (International) on Combustion, The Combustion Institute, Pittsburgh, PA, p. 1427 (1975).

12. Dobbins, R. A., Santoro, R. J. and Semerjian, H. G., Ed. T. D. McCay and J. A. Roux, Progress in Astronautics and Aeronautics, Vol. 92, p. 208 (1984).

13. Santoro, R. J., "Fuel Molecular Structure Effects on Soot Particle Growth in Diffusion Flames," Twentieth Fall Technical Meeting of the Eastern Section of the Combustion Institute, Gaithersburg, MD, Nov. 2-5, 1987.

14. Santoro, R. J., Yeh, T. T., Horvath, J. J. and Semerjian, H. G., Combustion Science and Technology, 53, p. 89 (1987).

15. Harris, S. J. and Weiner, A. M., Combustion Science and Technology, 31, 155 (1983).

16. Harris, S. J. and Weiner, A. M., Combustion Science and Technology, 32, 267 (1983).

17. Gomez, A., Sidebotham, G. and Glassman, I., Combustion and Flame, 58, 45 (1984).

5. PUBLICATIONS

1. Santoro, R. J., Yeh, T. T., Horvath, J. J. and Semerjian, H. G., "The Transport and Growth of Soot Particles in Laminar Diffusion Flames", Combustion Science and Technology, 53, 89 (1987).

2. Solomon, P. R., Best, P.E., Carangelo, R. M., Markham, J. R., Chien, P., Santoro, R. J. and Semerjian, H. G., "FT-IR Emission/Transmission Spectroscopy for In-Situ Combustion Diagnostics", Twenty-first Symposium (International) on Combustion, in press.

3. Santoro, R. J. and Miller, J. H., "Soot Particle Formation in Laminar Diffusion Flames", Langmuir, 3, p. 244-254 (1987).

4. Santoro, R. J., Horvath, J. J. and Semerjian, H. G., "Surface Growth Processes for Soot Particles in Diffusion Flames: Fuel Effects", to be submitted to Combustion and Flame.

6. MEETINGS AND PRESENTATIONS

1. "The Effect of Fuel Structure on the Formation and Growth of Soot Particles in Diffusion Flames", The Twenty-third Biennial Conference on Carbon, Worcester Polytechnic Institute, July 19-24, 1987.

2. "Soot Particle Formation in Diffusion Flames", American Chemical Society Symposium on Advances in Soot Chemistry, ASC Symposium, New Orleans, LA, August 30-September 4, 1987.

3. "Fuel Molecular Structure Effects on Soot Particle Growth in Diffusion Flames", Twentieth Fall Technical Meeting of the Eastern Section of the Combustion Institute, Gaithersburg, MD, November 2-5, 1987.

4. "Optical Measurements of Soot Particles in Flames", Materials Research Society Symposia, Reno, Nevada, April 5-8, 1988.

7. PARTICIPATING PROFESSIONALS

Dr. Robert J. Santoro, Associate Professor of Mechanical Engineering
Mr. Douglas McKensie, Graduate Student, Department of Mechanical Engineering
Mr. Jeff Leet, Graduate Student, Department of Mechanical Engineering

8. INTERACTIONS

A number of researchers have directly used the extensive data set developed as part of this work to compare with or extend their own research. Some of those who have been directly provided data include:

Professor R. A. Dobbins, Brown University, Providence, RI
Dr. R. Hall, United Technologies Research Center, East Hartford, CT
Dr. R. Davis, The National Bureau of Standards, Gaithersburg, MD
Dr. P. Solomon, Advanced Fuel Research, Inc., East Hartford, CT

In addition to the interactions resulting from interest in the soot particle data, there have been interactions with researchers on particle diagnostic problems. In some cases this has resulted in direct visits to particular laboratories to assist in solving these problems. These interactions include:

Dr. M. Zachariah, The National Bureau of Standards, Gaithersburg, MD
Ms. Valerie Lyons, NASA Lewis Research Center, Cleveland, OH

Several other interactions have also occurred through a general interest in the work supported by AFOSR with:

Columbian Chemical Company, Monroe, LA
Cummins Engine Company, Columbus, IN

END
DATED
FILM
8-88
DTIC